Development/Plasticity/Repair

Impaired Firing and Cell-Specific Compensation in Neurons Lacking $Na_v1.6$ Sodium Channels

Audra Van Wart and Gary Matthews
Graduate Program in Neuroscience, Department of Neurobiology and Behavior, State University of New York, Stony Brook, New York 11794-5230

The ability of neurons to fire precise patterns of action potentials is critical for encoding inputs and efficiently driving target neurons. At the axon initial segment and nodes of Ranvier, where nerve impulses are generated and propagated, a high density of $Na_v1.2$ sodium channels is developmentally replaced by $Na_v1.6$ channels. In retinal ganglion cells (GCs), this isoform switch coincides with the developmental transition from single spikes to repetitive firing. Also, $Na_v1.6$ channels are required for repetitive spiking in cerebellar Purkinje neurons. These previous observations suggest that the developmental appearance of $Na_v1.6$ underlies the transition to repetitive spiking in GCs. To test this possibility, we recorded from GCs of *med* ($Na_v1.6$-null) and wild-type mice during postnatal development. By postnatal day 18, when the switch to $Na_v1.6$ at GC initial segments is normally complete, the maximal sustained and instantaneous firing rates were lower in *med* than in wild-type GCs, demonstrating that $Na_v1.6$ channels are necessary to attain physiologically relevant firing frequencies in GCs. However, the firing impairment was milder than that reported previously in *med* Purkinje neurons, which prompted us to look for differences in compensatory sodium channel expression. Both $Na_v1.2$ and $Na_v1.1$ channels accumulated at initial segments and nodes of *med* GCs, sites normally occupied by $Na_v1.6$. In *med* Purkinje cells, only $Na_v1.1$ channels were found at initial segments, whereas in other brain regions, only $Na_v1.2$ was detected at *med* initial segments and nodes. Thus, compensatory mechanisms in channel isoform distribution are cell specific, which likely results in different firing properties.

Key words: **sodium channel; initial segment; retina; retinal ganglion cell; development; $Na_v1.6$**

Introduction

Voltage-gated sodium (Na_v) channels generate the rapidly rising phase of the action potential, as well as a number of subthreshold currents. There are 10 known Na_v α subunits, three of which are found predominantly in the postnatal CNS ($Na_v1.1$, $Na_v1.2$, and $Na_v1.6$). Each isoform has its own regional, cellular, and developmental expression in the nervous system (Trimmer and Rhodes, 2004), but the reasons for this isoform preference are largely unknown. $Na_v1.6$ channels appear to be particularly important, because they are the principal channels at axonal sites where action potentials are generated, namely the nodes of Ranvier and axon initial segments (ISs). Loss or disruption of $Na_v1.6$ channels in mice causes symptoms ranging from motor dysfunction and dystonia, to paralysis and juvenile [postnatal day 21 (P21)] lethality, suggesting that they are vital for impulse propagation later in life. However, why are $Na_v1.6$ channels the preferred channel at these sites?

When expressed in oocytes, α subunits $Na_v1.1$, $Na_v1.2$, and $Na_v1.6$ produce channels with subtle differences that are virtually eliminated when β subunits are coexpressed (Smith et al., 1998). However, recent data suggest that $Na_v1.6$ may have properties especially suited for repetitive or high-frequency firing. For example, when stimulated at high frequencies, $Na_v1.6$-mediated currents in oocytes show use-dependent potentiation (Zhou and Goldin, 2004), whereas $Na_v1.1$ and $Na_v1.2$ channels decrease in availability (Pugsley and Goldin, 1998; Spampanato et al., 2001), suggesting that $Na_v1.6$ channels may be more resistant to inactivation. Similar results were found in a neuronal expression system, in which $Na_v1.2$ channels showed greater accumulation of inactivation than $Na_v1.6$ channels during high-frequency stimulation (Rush et al., 2005). Furthermore, a specific role for $Na_v1.6$ in repetitive firing has been demonstrated in Purkinje neurons of the cerebellum. In mice lacking $Na_v1.6$ channels, Purkinje cells exhibit substantially reduced resurgent sodium current associated with rapid recovery from inactivation, resulting in loss of spontaneous firing, diminished repetitive firing abilities, and cell degeneration (Raman et al., 1997).

We examined the role of $Na_v1.6$ channels in the output neurons of the retina, the ganglion cells (GCs), which play the critical role of translating graded visual signals into a frequency code of action potentials. We showed previously that $Na_v1.2$ channels are clustered at early nodes and initial segments in GCs but that over development $Na_v1.6$ replaces $Na_v1.2$ as the predominant Na_v channel isoform at these sites (Boiko et al., 2003). Interestingly, this isoform transition coincides with the development of repetitive firing capability in these cells (Wang et al., 1997), which was

Received March 14, 2006; revised May 25, 2006; accepted May 31, 2006.

This work was supported by National Institutes of Health Grant EY03821 (G.M.) and National Research Service Award Fellowship F31 NS048762 (A.V.W.). We thank Drs. S. Rock Levinson (University of Colorado Medical School, Denver, CO), James S. Trimmer (University of California–Davis, Davis, CA), and Stephen Yazulla (State University of New York, Stony Brook, NY) for providing antibodies, and Dr. Miriam Meisler (University of Michigan, Ann Arbor, MI) for providing heterozygous *med*^{Tg} mice to start our colony. We thank Drs. Junryo Watanabe, Gail Mandel, James Salzer, James Trimmer, and Stephen Yazulla for helpful discussions.

Correspondence should be addressed to Gary Matthews, Department of Neurobiology and Behavior, Centers for Molecular Medicine, State University of New York, Stony Brook, NY 11794-5230. E-mail: gary.g.matthews@sunysb.edu.

DOI:10.1523/JNEUROSCI.1101-06.2006

 0270-6474/06/267172-09$15.00/0

attributed to faster recovery of Na_v channels from inactivation. Together with the demonstrated importance of $Na_v1.6$ in repetitive firing in Purkinje cells (Khaliq et al., 2003), this suggests that developmental expression of $Na_v1.6$ at the GC initial segment may account for the transition to repetitive spiking. Therefore, we compared the developmental progression of intrinsic firing abilities of GCs in $Na_v1.6$-null and wild-type (WT) mice to determine whether cells lacking $Na_v1.6$ exhibit impaired ability to fire repetitively.

Materials and Methods

Tissue preparation for immunohistochemistry. Animal use followed guidelines established by the National Institutes of Health and the Institutional Animal Care and Use Committee. Mice were killed using CO_2 at ages older than P14, and animals of postnatal ages P2–P14 were killed by rapid decapitation. Immediately after death, eyes and brains were dissected out and immersion fixed for 2 h on ice in freshly prepared 4% paraformaldehyde. For flat-mount preparation (Voigt and Wässle, 1987), retinas were processed free floating. For sections, retinas were hemisected, cryoprotected overnight at 4°C in 20% sucrose, frozen in M1 medium (Lipshaw, Pittsburgh, PA), and cryosectioned at 30 μm in a plane perpendicular to the surface of the retina.

Immunohistochemistry reagents. Flat mounts and cryosections were processed for immunohistochemistry as described previously (Van Wart et al., 2005). Pan-specific polyclonal (PAN) (Dugandzija-Novakovic et al., 1995) (gift from Dr. Rock Levinson, University of Colorado Medical School, Denver, CO) and monoclonal (K58/35) (Rasband et al., 1999) (gift from Dr. James S. Trimmer, University of California–Davis, Davis, CA) antibodies were generated against a conserved sequence present in all vertebrate Na_v1 isoforms. Anti-peptide rabbit polyclonal antibodies against the $Na_v1.2$ isoform were provided by Dr. James S. Trimmer and were developed against a unique sequence in the $Na_v1.2$ C terminus (Gong et al., 1999). Dr. Rock Levinson provided rabbit polyclonal antibodies against $Na_v1.6$, which were generated against a synthetic peptide corresponding to a unique sequence in the large intracellular domain I–II loop of $Na_v1.6$ (Caldwell et al., 2000). An anti-$Na_v1.1$ mouse monoclonal antibody (K74/71) was generated against a fusion protein consisting of the C terminus of rat $Na_v1.1$ and glutathione *S*-transferase carrier (Van Wart et al., 2005). A rabbit polyclonal anti-$Na_v1.1$ antibody was purchased from Chemicon (Temecula, CA). Mouse monoclonal anti-ankyrin-G (AnkG) antibody (clone 4G3F8) was purchased from Santa Cruz Biotechnology (Santa Cruz, CA). Anti-Caspr monoclonal (Rasband and Trimmer, 2001) and polyclonal (Boiko et al., 2001) antibodies were a gift from Dr. James S. Trimmer. Mouse anti-calbindin (Sigma, St. Louis, MO) was provided by Dr. Stephen Yazulla (State University of New York, Stony Brook, NY). Alexa 488-conjugated secondary antibodies (Invitrogen, Carlsbad, CA) were used to detect rabbit polyclonal antibodies, and cyanine 3-conjugated (Jackson Immunoresearch, West Grove, PA) or Alexa 568-conjugated (Invitrogen) secondary antibodies were used for visualization of the mouse monoclonal antibodies.

Confocal imaging. Images were acquired using a laser-scanning confocal microscope (FV-300; Olympus America, Center Valley, PA), initially processed using Olympus Optical FluoView software, and later exported into Adobe Photoshop 7.0 (Adobe Systems, San Jose, CA) for final processing. No staining above background was detectable in sections incubated with secondary antibody alone or with primary antibody preincubated with blocking peptide (data not shown). As indicated in the legends, figures show either planar projections of a series of successive confocal images or representative, individual confocal sections.

Transgenic animals. The *med*^{Tg} *Scn8a* (sodium channel, voltage gated, type VIII, α)-null mutation arose from a nontargeted transgene insertion on a C57BL/6J chromosome and has been maintained since 1992 by crossing to strain C57BL/6J (Burgess et al., 1995; Kohrman et al., 1995). A heterozygous breeding pair (gift from Dr. Miriam Meisler, University of Michigan, Ann Arbor, MI) was used to start a colony at State University of New York, Stony Brook. Wild-type C57BL/6 mice were obtained from Taconic Farms (Germantown, NY) and also used for breeding. Homozygous *med*^{Tg} mice could be recognized by their affected phenotypes (most notably progressive paralysis of the hindlimbs, with death by P21). Because of the high mortality of homozygous *med*^{Tg} mice between P19 and P21, experiments were typically performed on mice at ages P18 or younger. The genotypes of all mice were confirmed as follows. Genomic DNA was prepared from tail or ear snips by digestion with proteinase K, extraction with phenol/chloroform, and precipitation with ethanol. Genotypes were determined by PCR using 100 ng of genomic DNA and pairs of primers that amplify the mutant or the wild-type allele. Primer

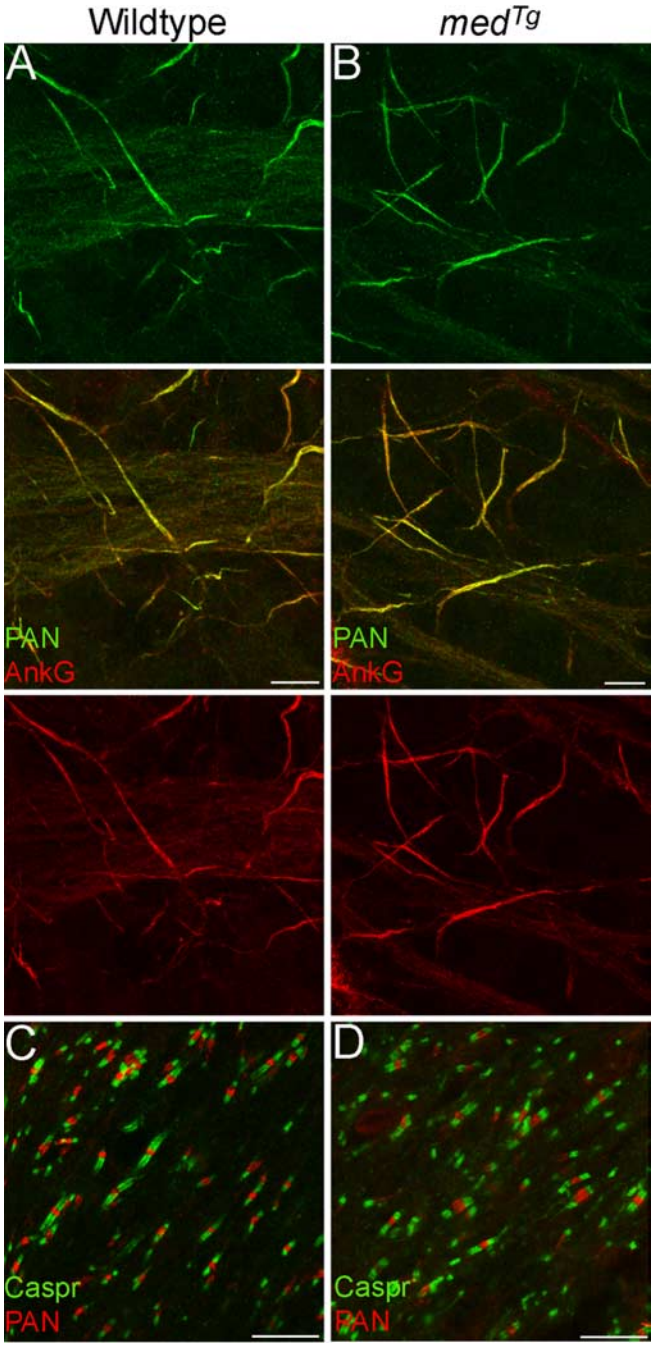

Figure 1. Na_v channel localization is normal in P18 *med*^{Tg} ($Na_v1.6$-null) mice. ***A***, ***B***, Wild-type (***A***) and $Na_v1.6$-null (***B***) P17 flat-mount retina stained with an antibody against AnkG (red) and a pan-specific sodium channel antibody (PAN, green). Projections through nerve fiber layer span 3 μm. In both genotypes, sodium channels cluster at high density at axon initial segments of GCs, which are marked by ankyrin-G immunoreactivity. ***C***, ***D***, Wild-type P20 (***C***) and $Na_v1.6$-null P21 (***D***) optic nerve stained for sodium channels (red) and the paranodal marker Caspr (green). Sodium channel localization appears normal at nodes of Ranvier in both WT and $Na_v1.6$-null optic nerves. Images span 4 μm. Scale bars, 10 μm.

pair 1 (forward, GAAGTGAAACCTTTAGACGAGCTGTATGAG; reverse, TTCTGGAAGTCGCCGTTCCTGTGAATGTCC) amplifies a 95 bp fragment from the wild-type *Scn8a* gene that is deleted by insertion of the transgene, spanning nucleotides 2356–2450 of the cDNA (Burgess et al., 1995) (GenBank U26707). Primer pair 2 (forward, AGGGAGGGCTGAGGGTTTGAAGTC; reverse, CCATGGTGTCTGTTTGAGGTTGCTA) amplifies a 243 bp product from the transgene. After denaturation for 3 min at 94°C, reactions were performed for 35 cycles of 45 s at 94°C, 45 s at 65°C, and 45 s at 72°C.

Tissue preparation for electrophysiology. Postnatal +/+, med^{Tg}/+, and med^{Tg}/med^{Tg} mouse pups were killed by rapid decapitation. Eyes were removed and hemisected through an incision along the ora serrata. Retinas were then freed from the pigment epithelium and subsequently stored in a chamber containing oxygenated Ames medium (Sigma) until the time of recording. The isolated retina was then placed in a recording chamber, ganglion cell layer up, and held in place by nylon strings strung across a platinum frame. The recording chamber was mounted on the stage of an upright microscope (Olympus America) equipped with a 60× water immersion lens. During recordings, the retina was continuously superfused with oxygenated Ames solution at a rate of 3 ml/min, and all recordings were performed at 33–37°C. Recordings were obtained during steady illumination of the retina, and visualization of cells was aided with an IPM-1000 Enpiction contrast enhancer (Enpiction Image Technologies, North Kingstown, RI). To access the ganglion cell layer, the vitreous, inner limiting membrane, and optic fiber layer were penetrated by applying positive pressure to the pipette. Only cells with a smooth surface and agranular appearance were targeted for recording. To differentiate ganglion cells from displaced amacrine cells, the largest accessible cell bodies in the field of view were targeted for recording, and data from cells that did not produce action potentials in response to depolarizing current were discarded (<4% of cells). Recordings were made from cells within the intermediate one-third of the retina. Recording sessions typically lasted 6 h, and viability of retinas was indicated by cell morphology, stable resting potentials, and the ability to evoke action potentials with depolarizing current injections.

Electrophysiological recordings. Whole-cell current-clamp recordings were made with an EPC9 patch-clamp amplifier (HEKA Elektronik, Lambrecht/Pfalz, Germany). Electrodes with tip resistances of 5–14 MΩ were prepared from borosilicate glass capillary tubing with filament (outer diameter of 1.5 mm, inner diameter of 0.86 mm; Warner Instruments, Hamden, CT) using a Flaming Brown Micropipette Puller (Sutter Instruments, Novato, CA). Recording electrodes were filled with a standard intracellular solution (pH 7.2) containing the following (in mM): 135 K gluconate, 10 HEPES, 10 KCl, 3 $MgCl_2$, 2 Na_2ATP, 0.5 GTP, and 0.2 K_2EGTA. Resting potentials were typically −54 to −60 mV, and, when necessary, cells were maintained at a holding potential of −60 mV by steady current injection. Input resistance was measured from the voltage change produced by 10–20 pA hyperpolarizing and depolarizing current pulses from a holding potential of −60 mV. To examine the firing properties, each cell was maintained in current-clamp mode and depolarized by injecting a series of positive current pulses of 1 s duration, beginning near threshold. Data were acquired with Pulse version 8.50 software (HEKA Elektronik) and exported to either Igor Pro (WaveMetrics, Lake Oswego, OR) or Excel (Microsoft, Seattle, WA) for final analysis.

Results

Sodium channel localization is normal in med^{Tg} animals

Homozygous med^{Tg} mice are null for $Na_v1.6$, resulting from a random transgene insertion into the *Scn8a* locus encoding $Na_v1.6$ (Burgess et al., 1995). Although these animals experience progressive paralysis of the hindlimbs and die by P21, this is sufficient time for GCs to make the transition to repetitive firing (Rothe et al., 1999) and for $Na_v1.6$ to be expressed at initial segments and nodes of Ranvier in WT cells (Boiko et al., 2003). The retinas of med^{Tg} mice have been reported to have no structural abnormalities (Buchner et al., 2004), and most animals do in fact open their eyes at the same age as their WT littermates, suggesting grossly normal eye development. To determine whether the localization of sodium channels at axon initial segments and nodes of Ranvier is normal in med^{Tg} mice, flat-mount retinas and optic nerve cryosections from WT versus med^{Tg} animals were stained using an antibody that recognizes all Na_v1 isoforms (PAN) and either the initial segment marker AnkG (Fig. 1*A*,*B*) or the paranodal marker Caspr (Fig. 1*C*,*D*). Sodium channel immunostaining at GC initial segments was indistinguishable in both genotypes (Fig. 1*A*,*B*), with intense sodium channel staining colocalized with ankyrin-G in the nerve fiber layer. Sections of optic nerve double labeled with PAN and the paranodal protein Caspr revealed bright PAN immunoreactivity at virtually all nodes of Ranvier in both genotypes (Fig. 1*C*,*D*). Furthermore, pan-specific sodium channel staining in the inner plexiform layer was also indistinguishable in WT and med^{Tg} retinas (data not shown). Therefore, the absence of $Na_v1.6$ channels does not substantially disrupt the overall targeting of Na_v1 isoforms in the retina or optic nerve.

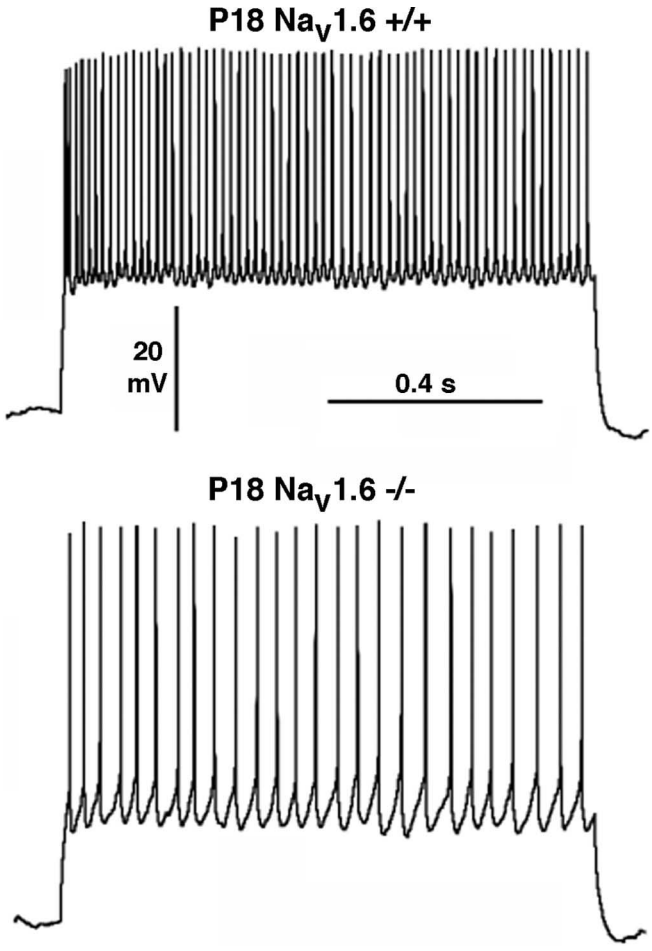

Figure 2. Both wild-type (+/+) and $Na_v1.6$-null (−/−) ganglion cells can support repetitive firing at P18 and encode a similar range of input intensities. Because of the high mortality rate beyond P18 (lethal by P21), this was the oldest age used for analysis. The traces show voltage recordings from one of the fastest cells from each genotype in response to a 60 pA current pulse lasting 1 s.

Repetitive firing is moderately disrupted in med^{Tg} GCs

Regardless of their functional classification (e.g., ON vs OFF, sustained vs transient responses to light), almost all adult GCs generate a sustained train of action potentials in response to depolarizing current (Wang et al., 1997; O'Brien et al., 2002). To

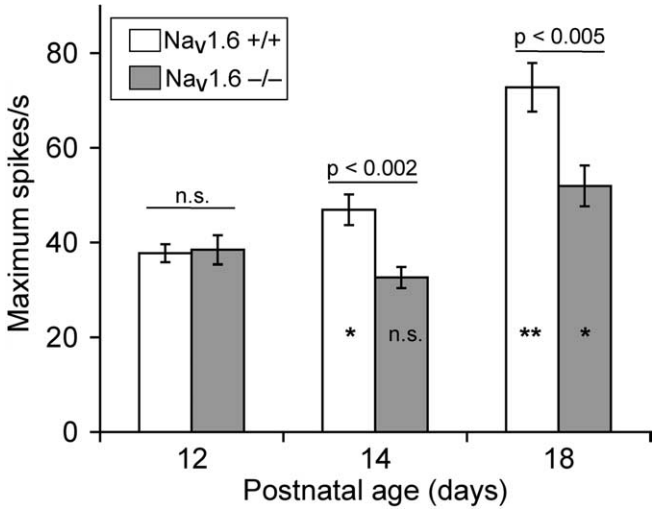

Figure 3. $Na_v1.6$-null GCs do not undergo the same developmental increase in firing rates as their wild-type counterparts. Developmental comparison of average sustained firing rates (maximum number of spikes fired during a 1 s current step). Only cells that reproducibly fired throughout the step were included (>90% of cells did so at all three ages). At P18, the average WT GC fired significantly more spikes during the pulse than the average med^{Tg} GC [73 vs 52 spikes/s, $p < 0.005$; an increase from the firing rate at P12 of 93% (WT) vs 35% (med^{Tg})]. At each age, the level of statistical significance of differences between WT (+/+) and med^{Tg} (−/−) cells is indicated above each pair of bars (n.s., not significant). The asterisks indicate the statistical significance of differences in firing rates for cells of each genotype at P14 and P18 compared with the same genotype at P12 (*$p < 0.03$; **$p < 0.001$).

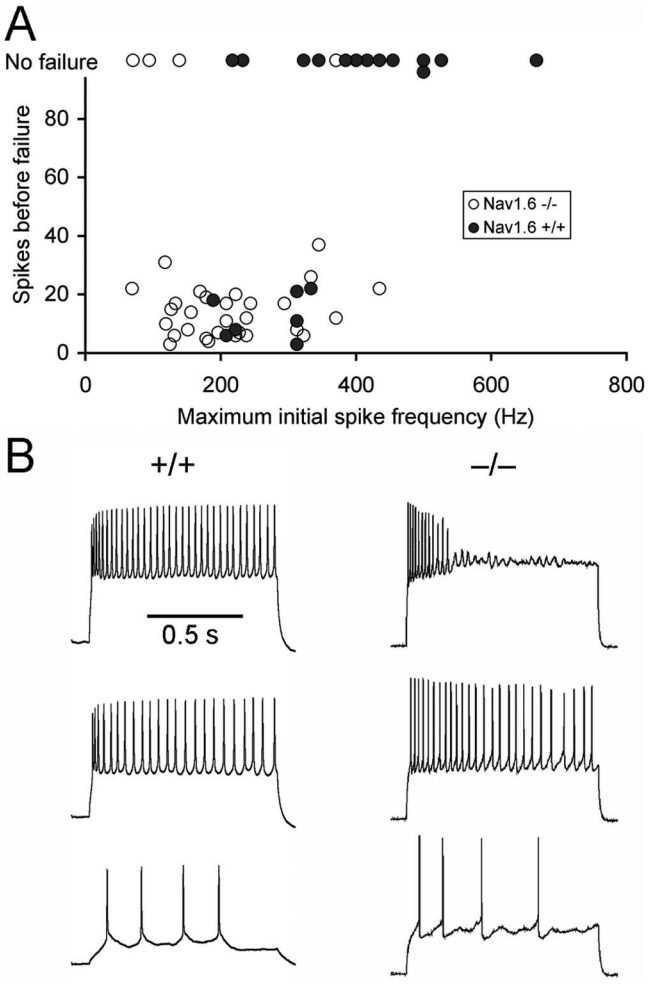

Figure 4. Wild-type GCs tend to have higher instantaneous spike frequencies and fewer failures when driven to these frequencies. ***A***, Each data point represents results from a single P18 WT GC (+/+; filled circles) or med^{Tg} GC (−/−; open circles). The position along the abscissa indicates the maximum instantaneous spike frequency (i.e., the reciprocal of the minimum interval between the first 2 spikes) observed for each cell. The ordinate indicates the number of spikes fired before failure during a 1 s depolarization at the level necessary to achieve the maximum instantaneous frequency. Instances in which the cell continued to fire throughout the 1 s depolarization are plotted along the top (No failure). ***B***, Examples of typical firing patterns of WT (left) and med^{Tg} (right) GCs in response to increasing depolarization, from levels just above threshold (bottom) to those required to reach maximum instantaneous frequency.

determine whether med^{Tg} GCs were also capable of sustained repetitive firing, we recorded action potentials triggered by depolarizing current steps in both WT and med^{Tg} GCs at age P18. To avoid damaging initial segments of GC axons, recordings were made using a flattened, intact retina preparation. Figure 2 shows examples from one of the fastest-firing cells from each group in response to a 60 pA current injection. Both WT and med^{Tg} GCs fired throughout the entire 1 s current pulse, although the maximal rate was lower in med^{Tg} GCs. On average, med^{Tg} GCs fired 52 ± 4 spikes during a 1 s depolarization ($n = 33$), which is significantly less than the 73 ± 5 spikes/s of WT GCs ($n = 25$; $p < 0.005$). Although significant, this impairment of repetitive firing is relatively subtle compared with the severe deficit in repetitive firing reported previously in cerebellar Purkinje cells of $Na_v1.6$-null mice (Raman et al., 1997; Khaliq et al., 2003). In the absence of $Na_v1.6$, Purkinje cells fire only one or two action potentials during sustained depolarizations (Khaliq et al., 2003), whereas we find that med^{Tg} GCs typically fire continuously (Fig. 2). Thus, unlike the med^{Tg} Purkinje neurons, the remaining repertoire of Na_v channels in med^{Tg} GCs is evidently able to compensate in large measure for the lack of $Na_v1.6$ channels and support repetitive spiking.

In developing rat retina, $Na_v1.2$ channels are found at early initial segments of GCs, before P7–P9, and are subsequently replaced by $Na_v1.6$ channels. By eye opening at P14, $Na_v1.6$ immunostaining is detected at 80% of GC initial segments (Boiko et al., 2003). Therefore, we expected that, if the impairment of repetitive firing observed at P18 in med^{Tg} GCs is in fact attributable to the absence of $Na_v1.6$ channels, then the impairment should be less apparent before eye opening, before the developmental appearance of $Na_v1.6$ in WT mice. To examine this, we recorded from WT and med^{Tg} GCs at age P12, just before the onset of visual activity. At this age, most mouse GCs are able to fire repetitively (Rothe et al., 1999), and the density of sodium current has reached adult levels in rat GCs (Schmid and Guenther, 1996, 1998). As shown in Figure 3, the maximum firing rate of WT and med^{Tg} GCs was indeed similar at P12 (WT, 38 ± 2 Hz, $n = 7$; med^{Tg}, 38 ± 3 Hz, $n = 14$). However, at P14, when $Na_v1.6$ is present at most GC initial segments (Boiko et al., 2003), WT GCs fired significantly more action potentials during a 1 s depolarization than age-matched med^{Tg} GCs (WT, 47 ± 3, $n = 17$; med^{Tg}, 33 ± 2, $n = 9$; $p < 0.002$) (Fig. 3). Between P12 and P18, WT GCs underwent a significant increase in maximal firing rate, rising 93% by P18 (WT P12 vs P18, $p < 10^{-6}$) (Fig. 3). Firing rates of GCs from med^{Tg} mice, conversely, did not increase as dramatically as their WT counterparts, with only a 35% elevation in firing rate between P12 and P18 (med^{Tg} P12 vs P18, $p < 0.02$) (Fig. 3). These data suggest that, although the remaining Na_v channel types in med^{Tg} GCs are able to support repetitive action potentials, the transition to $Na_v1.6$ channels at sites of spike generation may be required to achieve maximal sustained firing rates.

The pattern of results shown in Figure 3 could also be ex-

plained by a developmental delay in the $Na_v1.6$-null retina, so that GCs are less mature in med^{Tg} mice. However, there was no significant difference in input resistance at P18 between WT GCs (244 ± 24 MΩ) and med^{Tg} GCs (253 ± 23 MΩ; $p = 0.80$), which suggests that cells of the two genotypes were similar in size. Furthermore, the average current required to reach threshold (WT, 63 ± 11 pA; med^{Tg}, 78 ± 10 pA) and the average current required to reach maximum sustained firing rates (WT, 289 ± 40 pA; med^{Tg}, 261 ± 25 pA) were not significantly different between genotypes at P18 ($p = 0.29$, $p = 0.56$). Thus, both med^{Tg} and WT cells appear to encode a similar range of input intensities, albeit at different frequencies. However, the threshold for triggering action potentials averaged 4.2 mV more positive in med^{Tg} GCs than in wild-type cells ($p < 0.001$), which suggests that the density of sodium channels may be lower in med^{Tg} GCs.

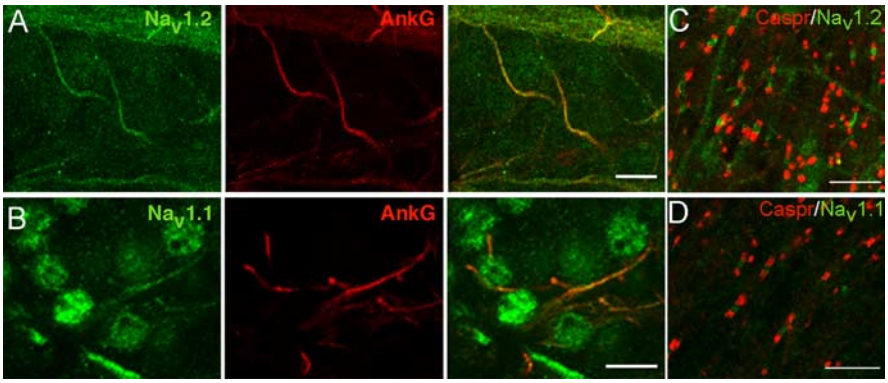

Figure 5. The remaining $Na_v1.1$ and $Na_v1.2$ channels in med^{Tg} GCs accumulate at sites normally occupied by $Na_v1.6$. P20 $Na_v1.6$-null retina and optic nerve. ***A***, Flat-mount retinas stained for $Na_v1.2$ and ankyrin-G. ***B***, Section of retina stained for $Na_v1.1$ and ankyrin-G. ***C***, ***D***, Optic nerve stained for Caspr and either $Na_v1.2$ or $Na_v1.1$. Both channel types are found throughout the ankyrin-G-defined initial segments, as well as at nodes of Ranvier. Images span 4 μm (***A***), 1 μm (***B***), 5 μm (***C***), 2 μm (***D***). Scale bars, 10 μm.

Mouse retinal ganglion cells fall into several morphometrically defined classes (Diao et al., 2004; Kong et al., 2005) that differ in soma size and dendritic arborization, and the comparable categories of GCs in cat retina differ in firing properties such as adaptation (O'Brien et al., 2002). Therefore, diversity in cell type within the sampled populations could affect the apparent differences in firing between WT and med^{Tg} GCs. In our recordings, we selectively targeted the largest somata in the GC layer, which biased the sampling in both WT and med^{Tg} retinas toward α ganglion cells, the subtype whose somata are largest (Völgyi et al., 2005). Indeed, the electrical properties of WT and med^{Tg} GCs were similar (see above), which suggests that the two sets of sampled cells were not grossly different. However, we did observe some variation in the rate and degree of adaptation within both sets of cells, and to reduce the possible influence of this variation on comparisons between WT and med^{Tg} GCs, we focused on the instantaneous spike frequency at the onset of depolarization.

Lack of $Na_v1.6$ reduces instantaneous frequency and promotes spike failure

In the intact retina, ganglion cells are typically driven to fire by short-lasting synaptic depolarizations that trigger a rapid burst of a few action potentials (Zaghloul et al., 2003). The short interval between spikes in a burst increases the efficacy of GCs in directly driving thalamic relay neurons in the dorsal lateral geniculate nucleus (Usrey et al., 1998) and polysynaptically driving simple cells in layer IV of visual cortex (Kara and Reid, 2003). Thus, the ability to fire a few action potentials rapidly at the onset of depolarization is likely to be of substantial functional significance for retinal ganglion cells. To examine this, we asked how closely together a cell is capable of firing two action potentials at the onset of depolarization. With increasing depolarization, the interval between the first and second spikes typically decreases progressively, until the minimum achievable interspike interval is reached. The reciprocal of this interval is the maximum instantaneous spike frequency, which is plotted along the abscissa in Figure 4*A* for GCs from WT mice (filled circles) and med^{Tg} mice (open circles) at age P18. In WT GCs, the maximum achievable frequency averaged 367 ± 23 spikes/s ($n = 23$), which was significantly higher than med^{Tg} GCs (211 ± 15 spikes/s; $n = 35$; $p < 10^{-5}$). Therefore, GCs lacking $Na_v1.6$ are less able to generate spikes at short interspike intervals at the onset of depolarization, which may reduce their transmission efficacy at later synaptic stages in the visual system. The peak rate we found for WT GCs is comparable with the maximum rate of 300–500 spikes/s observed during light responses of brisk-type ganglion cells in intact mammalian retina (DeVries and Baylor, 1997; Koch et al., 2004), which indicates that the deficit exhibited by med^{Tg} GCs is likely physiologically relevant.

At the level of depolarization necessary to achieve the maximum instantaneous frequency, WT GCs usually continued to fire robustly throughout a 1 s current pulse without spike failure, as illustrated in Figure 4*B* (left top panel). Instances of such continuous firing are indicated by "No failure" on the ordinate in Figure 4*A*. In contrast, once the maximum initial frequency was achieved, GCs from med^{Tg} mice commonly fired only 5–30 spikes before failure (Fig. 4*A*,*B*, right top panel). Thus, not only were WT cells capable of firing faster, but they were also able to sustain spiking longer when driven to maximum instantaneous firing rates.

Differential Na_v channel isoform distribution in med^{Tg} cells

Although $Na_v1.6$ channels are important for high-frequency firing in GCs, other Na_v channels partially compensated for the lack of $Na_v1.6$. Therefore, we next examined the distribution of the remaining $Na_v1.1$ and $Na_v1.2$ channels in sections of retina and optic nerve. As in adults, the predominant channel of initial segments and nodes in WT P18 mice was $Na_v1.6$, whereas $Na_v1.2$ was found distributed uniformly along GC axons (data not shown). Consistent with the fact that the isoform switch from $Na_v1.2$ to $Na_v1.6$ at optic nerve nodes is not yet complete at this age (Boiko et al., 2001), $Na_v1.2$ was also detected at a number of nodes of Ranvier in the P18 WT animals.

We showed in Figure 1 that Na_v channels are in fact clustered at med^{Tg} GC initial segments and at all nodes in the med^{Tg} optic nerve. We also showed previously that $Na_v1.1$ channels occupy a subregion in the proximal portion of the GC initial segment during week 3 of development in WT animals, but $Na_v1.1$ channels were not detected in WT nodes of Ranvier (Van Wart et al., 2004, 2005). With this in mind, we examined whether the remaining Na_v channels at nodes and initial segments of med^{Tg} mice would be the $Na_v1.1$ channels of the proximal initial segment or the $Na_v1.2$ channels found earlier in development. In flat-mount ret-

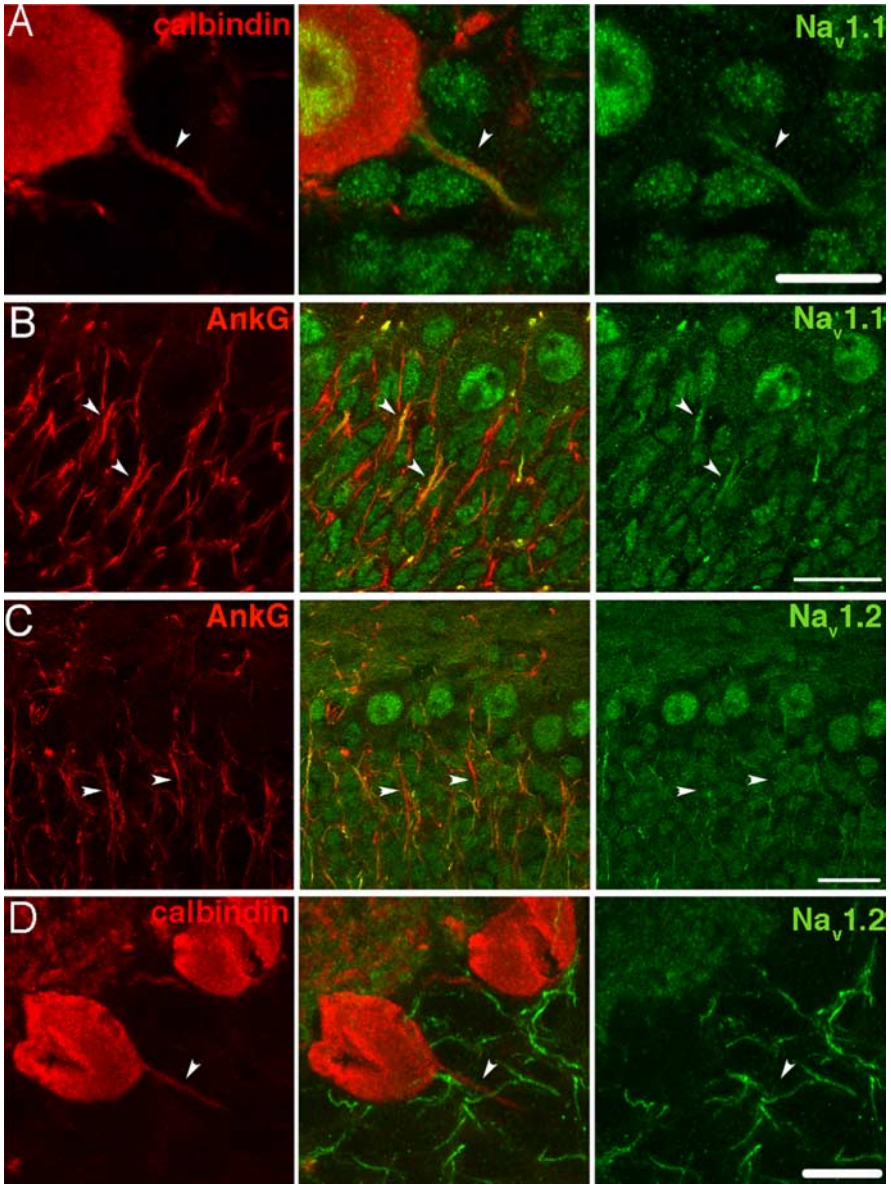

Figure 6. Cerebellar Purkinje neurons of $Na_v1.6$-null animals express $Na_v1.1$ but not $Na_v1.2$ at their axon initial segments. Sections of P20 med^{Tg} cerebellum stained with anti-$Na_v1.1$ (***A***, ***B***; green) or anti-$Na_v1.2$ antibody (***C***, ***D***; green), together with immunostaining for either ankyrin-G to mark initial segments (***B***, ***C***; red), or the Purkinje cell marker calbindin (***A***, ***D***; red). ***A***, Arrowhead indicates the initial segment of a calbindin-labeled Purkinje cell, with an associated cluster of $Na_v1.1$ immunoreactivity. Calbindin-negative cells lack $Na_v1.1$ immunostaining. ***B***, Arrowheads indicate two examples of large initial segments that are positive for both ankyrin-G and $Na_v1.1$ channels. Numerous smaller initial segments likely originate from cerebellar granule cells and lack detectable $Na_v1.1$ immunofluorescence. ***C***, $Na_v1.2$ antibody labels most initial segments in the granule cell layer but does not label large initial segments (arrowheads) near Purkinje cell bodies. ***D***, $Na_v1.2$ immunostaining is not detectable in axon initial segments (e.g., arrowhead) of Purkinje cells labeled with anti-calbindin. Images are projections of confocal *Z*-series spanning 4 μm (***A***), 3 μm (***B***), 8 μm (***C***), or 5 μm (***D***). Scale bars: ***A***, ***D***, 10 μm; ***B***, ***C***, 20 μm.

which $Na_v1.1$ channels cluster only in the most proximal one-third of the initial segment, with $Na_v1.6$ channels occupying the more distal two-thirds (Van Wart et al., 2004). Therefore, both $Na_v1.1$ and $Na_v1.2$ channels accumulate in place of the missing $Na_v1.6$ channels in the distal IS of med^{Tg} mice. Furthermore, although $Na_v1.1$ channels are normally not found in the WT myelinated optic nerve at any point in development, $Na_v1.1$ staining was detectable at a number of optic nerve nodes in P21 med^{Tg} animals (Fig. 5*D*). Thus, when $Na_v1.6$ is lacking, both $Na_v1.1$ and $Na_v1.2$ channels are distributed to the appropriate membrane domains to partially compensate for the missing $Na_v1.6$ channels. These findings not only highlight the importance of these domains for effective signal propagation but also show that other sodium channel types are able to cluster at sites from which they would normally be excluded. Perhaps it is this ability of GCs that accounts for the difference in repetitive firing capability between GCs and cerebellar Purkinje neurons of med^{Tg} mice.

Like GCs of the retina, the Purkinje cells of the cerebellum express $Na_v1.1$, $Na_v1.2$, and $Na_v1.6$ channels, with $Na_v1.6$ but not $Na_v1.1$ normally clustered at adult initial segments (Jenkins and Bennett, 2001; Van Wart et al., 2004). Because cerebellar Purkinje cells of med^{Tg} mice have been reported to have more severe deficits in repetitive firing than we observed in GCs, we examined the compensatory changes in Na_v channel expression at Purkinje cell initial segments of $Na_v1.6$-null mice. In sections of cerebellum from P21 med^{Tg} animals, labeled with anti-calbindin as a Purkinje-cell marker, $Na_v1.1$ immunostaining was present at Purkinje cell initial segments (Fig. 6*A*), in which it is not normally found. Ankyrin-G staining also colocalized with these $Na_v1.1$-positive segments near the Purkinje cell bodies, confirming that these sites are initial segments (Fig. 6*B*, arrowheads). In addition, Figure 6*B* also shows numerous ankyrin-G-positive initial segments, probably arising from granule cells, that are not positive for $Na_v1.1$ channels. Because $Na_v1.2$ channels are found at GC initial segments of med^{Tg} mice, we examined whether $Na_v1.2$ channels account for Na_v clustering at the $Na_v1.1$-negative initial segments in the granule cell layer and possibly at Purkinje cell initial segments in addition to the $Na_v1.1$ channels shown in Figure 6*A*. As shown in Figure 6*C*, most ankyrin-G sites in the granule cell layer colocalize with $Na_v1.2$, which suggests that initial segments of granule cells contain $Na_v1.2$ but not $Na_v1.1$ channels. However, a few large ankyrin-G-positive initial segments were devoid of $Na_v1.2$ immunostaining (Fig. 6*C*, arrowheads). To determine whether these $Na_v1.2$-negative initial segments belong to Purkinje cells,

inas from P18 med^{Tg} animals stained for $Na_v1.2$ and ankyrin-G, $Na_v1.2$ immunostaining was observed in the GC axon fascicles and cell bodies, as well as at ankyrin-G-labeled initial segments and a large percentage of Caspr-flanked nodes of Ranvier (Fig. 5*A*,*C*). Thus, $Na_v1.2$ channels, which are sequestered to newly forming nodes of Ranvier and initial segments early in development (Boiko et al., 2001, 2003), remain at these sites when $Na_v1.6$ is not present. In sections of retina stained for $Na_v1.1$ and ankyrin-G (Fig. 5*B*), $Na_v1.1$ channels were also found at initial segments, extending throughout the ankyrin-G-labeled region. This differs from the normal pattern in WT initial segments, in

we double labeled sections of P21 med^{Tg} cerebellum with anti-calbindin and anti-$Na_v1.2$. Although $Na_v1.2$ channels were present at numerous calbindin-negative sites, which likely represent initial segments of granule cells (Fig. 6*C*), no $Na_v1.2$ immunoreactivity was detectable in initial segments of Purkinje cells (Fig. 6*D*, arrowhead). Therefore, we conclude that initial segments of med^{Tg} Purkinje cells express $Na_v1.1$ but not $Na_v1.2$, whereas the reverse is true for initial segments of cerebellar granule cells.

In the optic nerve of med^{Tg} mice, we detected both $Na_v1.1$ and $Na_v1.2$ channels at nodes of Ranvier in lieu of the missing $Na_v1.6$ channels. We also observed puncta of $Na_v1.1$ immunostaining, which likely represent nodes of Ranvier, in calbindin-stained axons of Purkinje cells descending through the granule cell layer (Fig. 7*A*,*B*). Focal clusters of $Na_v1.2$ immunoreactivity were not observed in association with calbindin-positive axons of Purkinje cells (data not shown). In cerebellar white matter stained with anti-ankyrin-G to reveal nodes of Ranvier, bright clusters of $Na_v1.1$ immunostaining colocalized with ankyrin-G (Fig. 7*C*), especially at larger clusters that likely correspond to nodes of large-diameter axons of Purkinje cells (Fig. 7*C*, arrows indicate examples of ring-like staining at large transversely sectioned nodes). Smaller ankyrin-G-positive nodes in the cerebellar white matter, which probably represent axons of cells other than Purkinje cells, were not positive for $Na_v1.1$ (Fig. 7*C*) but were positive for $Na_v1.2$ (data not shown). Therefore, $Na_v1.1$ apparently takes the place of $Na_v1.6$ at both initial segments and nodes of Purkinje-cell axons. However, this pattern was not repeated in other parts of the med^{Tg} brain we examined. For example, in cerebral cortex (Fig. 8*A*) and hippocampus (Fig. 8*B*), $Na_v1.2$ but not $Na_v1.1$ channels (data not shown) were found at initial segments that would normally contain $Na_v1.6$. Additionally, unlike Purkinje cells, $Na_v1.2$ was detected at nodes of Ranvier in white matter of other parts the med^{Tg} brain, such as the corpus callosum (Fig. 8*C*). Overall, $Na_v1.2$ channels typically replace missing $Na_v1.6$ channels at nodes and initial segments of med^{Tg} brain neurons, whereas $Na_v1.1$ channels are found at these sites in Purkinje cells. Retinal ganglion cells exhibit a third pattern, having both $Na_v1.1$ and $Na_v1.2$ channels at axonal sites normally occupied by $Na_v1.6$. Thus, various compensatory mechanisms are apparently used in different neurons, which may account for their distinct firing capabilities in the absence of $Na_v1.6$ channels.

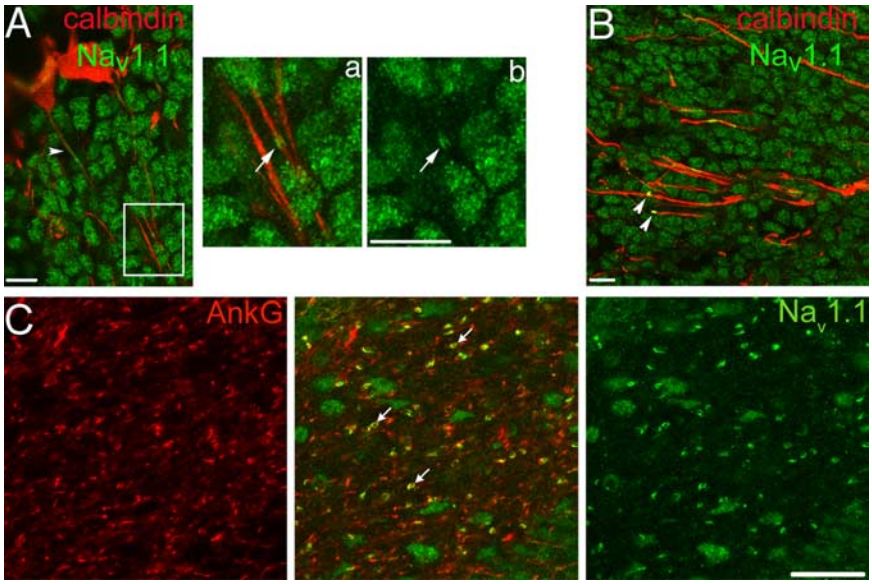

Figure 7. $Na_v1.1$ channels are located at nodes of Ranvier in the cerebellum of $Na_v1.6$-null mice. Sections of P20 med^{Tg} cerebellum stained with $Na_v1.1$ antibody (green) and either anti-calbindin (***A***, ***B***; red) or ankyrin-G antibody (***C***; red). ***A***, ***B***, $Na_v1.1$ immunostaining is associated with calbindin-labeled axons of Purkinje cells at the initial segment (***A***, arrowhead) and at focal spots deeper in the granule-cell layer (box, ***A***; arrowheads, ***B***). Insets ***a*** and ***b*** show a higher-magnification view of the region indicated by the box in ***A***, to illustrate a focal spot of $Na_v1.1$ immunofluorescence associated with the axon membrane (arrows). ***C***, Nodes of Ranvier in the cerebellar white matter marked with anti-ankyrin-G (red). Focal spots of $Na_v1.1$ immunofluorescence colocalize with ankyrin-G immunostaining (middle, yellow). Images are projections of confocal *Z*-series spanning 3 μm (***A***, ***C***) or 4 μm (***B***). Scale bars: ***A***, ***B***, 10 μm; ***C***, 20 μm.

Discussion

A role for $Na_v1.6$ in high-frequency firing

We find that med^{Tg} retinal ganglion cells lacking sodium channel $Na_v1.6$ exhibit deficits in high-frequency firing compared with their wild-type counterparts, including lower instantaneous spike frequency at the onset of depolarization and reduced maximal frequency and more rapid spike failure during sustained depolarization. Moreover, these differences emerge during the developmental period when $Na_v1.6$ channels replace $Na_v1.2$ channels at the axon initial segment of wild-type GCs. Therefore, we suggest that the presence of $Na_v1.6$ channels promotes both high instantaneous spike frequency and resistance to failure during sustained firing. What qualities of $Na_v1.6$ make it important for supporting the higher firing frequencies seen in wild-type retinas? Previous studies have demonstrated reduced availability of $Na_v1.1$ and $Na_v1.2$ channels during repetitive stimulation at high frequency compared with $Na_v1.6$ channels (Pugsley and Goldin, 1998; Spampanato et al., 2001; Zhou and Goldin; 2004; Rush et al., 2005), which suggests that $Na_v1.6$ channels recover from inactivation more rapidly and hence promote faster repetitive firing. More rapid recovery from inactivation by $Na_v1.6$ channels might also influence the time course and degree of spike-frequency adaptation in GCs, which is governed at least in part by sodium channel inactivation (Kim and Rieke, 2003). In addition to the transient current that underlies the action potential, heterologously expressed $Na_v1.6$ channels also mediate a larger persistent (non-inactivating) current than $Na_v1.1$ or $Na_v1.2$ (Smith et al., 1998; Rush et al., 2005). This persistent current is larger at more positive potentials (Smith et al., 1998) and is highly reduced in neurons lacking $Na_v1.6$ (Raman et al., 1997; Maurice et al., 2001; Do and Bean, 2004). Thus, $Na_v1.6$-dependent persistent current may promote interspike depolarization and repetitive spiking in normal GCs but not in $Na_v1.6$-null med^{Tg} GCs.

Isoform-specific modulation of Na_v channels may also affect firing rates in neurons. For example, calmodulin differentially modulates $Na_v1.6$ inactivation kinetics and current density (Herzog et al., 2003). Additionally, although $Na_v1.6$ does impart specific sodium-current kinetics in cerebellar Purkinje neurons, other isoforms behave similarly if properly modulated. For instance, resurgent current like that mediated by $Na_v1.6$ in Purkinje cells can also be generated by other α subunits when their inactivation is slowed pharmacologically (Grieco and Raman, 2004). Furthermore, although β subunits have been shown to make the

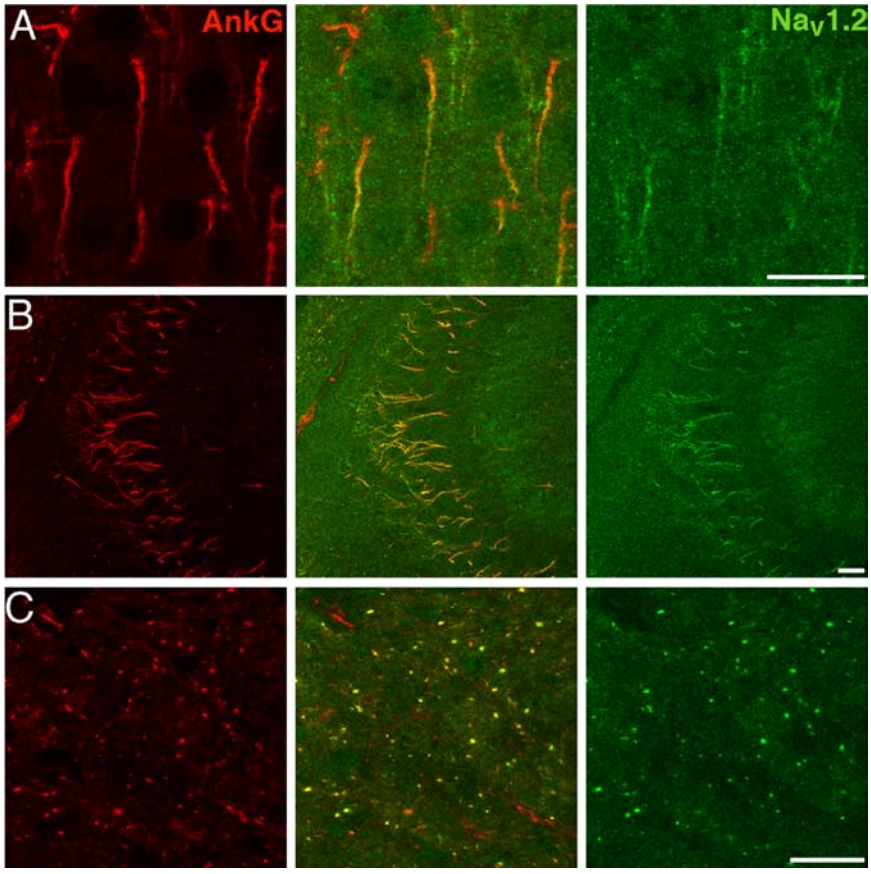

Figure 8. $Na_v1.2$ is found at initial segments and nodes of Ranvier in the cortex, hippocampus, and corpus callosum of $Na_v1.6$-null mice. Sections of P20 med^{Tg} brain stained with antibodies against ankyrin-G (red) and $Na_v1.2$ (green). Extensive colocalization of immunofluorescence is seen at initial segments of neurons in the cortex (***A***) and area CA2/3 of the hippocampus (***B***), as well as virtually all nodes of Ranvier in the corpus callosum (***C***). $Na_v1.1$ immunoreactivity is not detectable at any of these sites (data not shown). Images span 7 μm (***A***), 8 μm (***B***), and 4 μm (***C***). Scale bars, 20 μm.

properties of $Na_v1.1$, $Na_v1.2$, and $Na_v1.6$ channels even more similar (Smith et al., 1998), the recently discovered β4 subunit has been suggested to provide the open-channel block necessary for resurgent current, and it can induce resurgence in neurons in which it is not normally expressed (Grieco et al., 2005). Interestingly, resurgent sodium current is reduced but not absent in neurons of the subthalamic nucleus in mice lacking $Na_v1.6$ (Do and Bean, 2004). Thus, cell-specific differences in the modulation of remaining Na_v channel isoforms may explain why some neural systems in med^{Tg} animals are less affected by the absence of $Na_v1.6$.

Channel compensation in retinal ganglion cells and other CNS neurons

Although med^{Tg} GCs do show deficits in maximum firing rates, the remaining $Na_v1.2$ and $Na_v1.1$ channels in these cells compensate reasonably well for the lack of $Na_v1.6$. The mutant GCs do undergo a developmental increase in repetitive firing, albeit less so than wild-type cells, and $Na_v1.1$ and $Na_v1.2$ channels localize to nodes of Ranvier and initial segments, both of which are sites normally occupied by $Na_v1.6$. Sodium channels in GC dendrites can also initiate spikes (Velte and Masland, 1999; Oesch et al., 2005), and dendritic Na_v channels might also contribute to the ability of GCs to fire repetitively in the absence of $Na_v1.6$. However, sodium channel immunoreactivity in GC dendrites is sparse and difficult to detect, which suggests that the high density of $Na_v1.1$ and $Na_v1.2$ channels at the initial segment would likely be the more important determinant of firing properties in med^{Tg} GCs.

In cerebellar Purkinje cells of $Na_v1.6$-null mice, the absence of $Na_v1.6$ results in loss of spontaneous firing and more severe defects in repetitive firing than we observed in GCs (Raman et al., 1997; Khaliq et al., 2003). Interestingly, we found that, unlike med^{Tg} GCs, cerebellar Purkinje neurons of med^{Tg} mice do not retain $Na_v1.2$ at their initial segments during postnatal development, nor are $Na_v1.2$ channels detected in their somata by immunofluorescence. Instead, $Na_v1.1$ channels take the place normally occupied by $Na_v1.6$ at the Purkinje cell initial segment. Although the reported loss of resurgent current in Purkinje cells appears to be the main cause of their firing deficits (Raman et al., 1997; Khaliq et al., 2003; Do and Bean, 2004), the severity of the Purkinje-cell phenotype is likely enhanced by apparent absence of $Na_v1.2$, as well as $Na_v1.6$.

Unlike Purkinje cells, most neurons elsewhere in the med^{Tg} brain respond to the lack of $Na_v1.6$ by expressing $Na_v1.2$, but not $Na_v1.1$, at initial segments and nodes of Ranvier. Thus, it appears that compensatory Na_v channel localization varies among CNS cell types. It is not yet clear how this differential expression influences the physiology of other cell types and how this affects the overall phenotype of the animal. Although, the major dysfunction of med^{Tg} mice is in motor capabilities (Burgess et al., 1995), recent studies have suggested that humans heterozygous for an Scn8a truncation allele, as well as mice heterozygous for $Na_v1.6$ mutation, also have cognitive deficits (McKinney et al., 2005; Trudeau et al., 2005). However, electrophysiological studies have shown that the voltage-dependent properties of Na_v channels in prefrontal cortical neurons from $Na_v1.6$-null mice are indistinguishable from wild type, although transient and persistent current in those cells is reduced (Maurice et al., 2001). Furthermore, whereas some neurons involved in motor pathways have severe firing deficits in $Na_v1.6$-null mice, such as cerebellar Purkinje cells (Raman and Bean, 1997) and mesencephalic trigeminal neurons (Enomoto et al., 2005), no difference was found in the frequency of spontaneous or current-driven firing in subthalamic nuclear neurons (Do and Bean, 2004). The mechanisms underlying this variation in compensatory abilities among individual cell types, and the correlation between channel distribution and residual function, require additional study.

During normal optic nerve development, $Na_v1.2$ channels remain at nodes of Ranvier until $Na_v1.6$ channels appear (Boiko et al., 2001), and, in the *medJ* $Na_v1.6$-hypomorph, $Na_v1.2$ retention at nodes is prolonged until enough $Na_v1.6$ channels are synthesized (Kearney et al., 2002). Thus, it is perhaps not surprising that $Na_v1.2$ channels are retained at nodes and initial segments of med^{Tg} animals. However, we were surprised to find an accumulation of $Na_v1.1$ channels at med^{Tg} nodes of Ranvier, in light of their absence from WT optic nerve nodes throughout development. Furthermore, whereas $Na_v1.1$ channels normally accumulate

in a short region of the proximal IS but not in the distal IS (Van Wart et al., 2004), they are distributed throughout the ankyrin-G-labeled IS in *med*^{Tg} GCs. Thus, both $Na_v1.2$ and $Na_v1.1$ channels interact with the same clustering machinery and targeting systems as $Na_v1.6$, and the mechanisms that restrict their localization in adults apparently require the presence of $Na_v1.6$.

References

Boiko T, Rasband MN, Levinson SR, Caldwell JH, Mandel G, Trimmer JS, Matthews G (2001) Compact myelin dictates the differential targeting of two sodium channel isoforms in the same axon. Neuron 30:91–104.

Boiko T, Van Wart A, Caldwell JH, Levinson SR, Trimmer JS, Matthews G (2003) Functional specialization of the axon initial segment by isoform-specific sodium channel targeting. J Neurosci 23:2306–2313.

Buchner DA, Seburn KL, Frankel WN, Meisler MH (2004) Three ENU-induced neurological mutations in the pore loop of sodium channel Scn8a (Na_v 1.6) and a genetically linked retinal mutation, rd13. Mamm Genome 15:344–351.

Burgess DL, Kohrman DC, Galt J, Plummer NW, Jones JM, Spear B, Meisler MH (1995) Mutation of a new sodium channel gene, Scn8a, in the mouse mutant "motor endplate disease." Nat Genet 10:461–465.

Caldwell JH, Schaller KL, Lasher RS, Peles E, Levinson SR (2000) Sodium channel Na_v 1.6 is localized at nodes of Ranvier, dendrites, and synapses. Proc Natl Acad Sci USA 97:5616–5620.

DeVries SH, Baylor DA (1997) Mosaic arrangement of ganglion cell receptive fields in rabbit retina. J Neurophysiol 78:2048–2060.

Diao L, Sun W, Deng Q, He S (2004) Development of the mouse retina: emerging morphological diversity of the ganglion cells. J Neurobiol 61:236–249.

Do MT, Bean BP (2004) Sodium currents in subthalamic nucleus neurons from $Na_v1.6$-null mice. J Neurophysiol 92:726–733.

Dugandzija-Novakovic S, Koszowski AG, Levinson SR, Shrager P (1995) Clustering of Na^+ channels and node of Ranvier formation in remyelinating axons. J Neurosci 15:492–503.

Enomoto A, Han JM, Hsiao C, Chandler SH (2005) Sodium currents in mesencephalic trigeminal neurons of $Na_v1.6$-null mice. Soc Neurosci Abstr 31:151.4.

Gong B, Rhodes KJ, Bekele-Arcuri Z, Trimmer JS (1999) Type I and type II Na^+ channel alpha-subunit polypeptides exhibit distinct spatial and temporal patterning, and association with auxiliary subunits in rat brain. J Comp Neurol 412:342–352.

Grieco TM, Raman IM (2004) Production of resurgent current in $Na_v1.6$-null Purkinje neurons by slowing sodium channel inactivation with β-pompilidotoxin. J Neurosci 24:35–42.

Grieco TM, Malhotra JD, Chen C, Isom LL, Raman IM (2005) Open-channel block by the cytoplasmic tail of sodium channel β4 as a mechanism for resurgent sodium current. Neuron 45:233–244.

Herzog RI, Liu C, Waxman SG, Cummins TR (2003) Calmodulin binds to the C terminus of sodium channels $Na_v1.4$ and $Na_v1.6$ and differentially modulates their functional properties. J Neurosci 23:8261–8270.

Jenkins SM, Bennett V (2001) Ankyrin-G coordinates assembly of the spectrin-based membrane skeleton, voltage-gated sodium channels, and L1 CAMs at Purkinje neuron initial segments. J Cell Biol 155:739–746.

Kara P, Reid RC (2003) Efficacy of retinal spikes in driving cortical responses. J Neurosci 23:8547–8557.

Kearney JA, Buchner DA, De Haan G, Adamska M, Levin SI, Furay AR, Albin RL, Jones JM, Montal M, Stevens MJ, Sprunger LK, Meisler MH (2002) Molecular and pathological effects of a modifier gene on deficiency of the sodium channel Scn8a (Na_v 1.6). Hum Mol Genet 11:2765–2775.

Khaliq ZM, Gouwens NW, Raman IM (2003) The contribution of resurgent sodium current to high-frequency firing in Purkinje neurons: an experimental and modeling study. J Neurosci 23:4899–4912.

Kim KJ, Rieke F (2003) Slow Na^+ inactivation and variance adaptation in salamander retinal ganglion cells. J Neurosci 23:1506–1516.

Koch K, McLean J, Berry M, Sterling P, Balasubramanian V, Freed MA (2004) Efficiency of information transmission by retinal ganglion cells. Curr Biol 14:1523–1530.

Kohrman DC, Plummer NW, Schuster T, Jones JM, Jang W, Burgess DL, Galt J, Spear BT, Meisler MH (1995) Insertional mutation of the motor endplate disease (med) locus on mouse chromosome 15. Genomics 26:171–177.

Kong JH, Fish DR, Rockhill RL, Masland RH (2005) Diversity of ganglion cells in the mouse retina: unsupervised morphological classification and its limits. J Comp Neurol 489:293–310.

Maurice N, Tkatch T, Meisler M, Sprunger LK, Surmeier DJ (2001) D_1/D_5 dopamine receptor activation differentially modulates rapidly inactivating and persistent sodium currents in prefrontal cortex pyramidal neurons. J Neurosci 21:2268–2277.

McKinney BC, Meisler MH, Murphy GG (2005) Cognitive and behavioral abnormalities in mice heterozygous for a null mutation in sodium channel *Scn8a*. Soc Neurosci Abstr 31:196.12.

O'Brien BJ, Isayama T, Richardson R, Berson DM (2002) Intrinsic physiological properties of cat retinal ganglion cells. J Physiol (Lond) 538:787–802.

Oesch N, Euler T, Taylor WR (2005) Direction-selective dendritic action potentials in rabbit retina. Neuron 47:739–750.

Pugsley MK, Goldin AL (1998) Time- and voltage-dependent block of sodium channels expressed in *Xenopus* oocytes by RSD 921, a novel class I antiarrhythmic drug. Proc West Pharmacol Soc 41:75–76.

Raman IM, Bean BP (1997) Resurgent sodium current and action potential formation in dissociated cerebellar Purkinje neurons. J Neurosci 17:4517–4526.

Raman IM, Sprunger LK, Meisler MH, Bean BP (1997) Altered subthreshold sodium currents and disrupted firing patterns in Purkinje neurons of Scn8a mutant mice. Neuron 19:881–891.

Rasband MN, Trimmer JS (2001) Subunit composition and novel localization of K^+ channels in spinal cord. J Comp Neurol 429:166–176.

Rasband MN, Peles E, Trimmer JS, Levinson SR, Lux SE, Shrager P (1999) Dependence of nodal sodium channel clustering on paranodal axoglial contact in the developing CNS. J Neurosci 19:7516–7528.

Rothe T, Bahring R, Carroll P, Grantyn R (1999) Repetitive firing deficits and reduced sodium current density in retinal ganglion cells developing in the absence of BDNF. J Neurobiol 40:407–419.

Rush AM, Dib-Hajj SD, Waxman SG (2005) Electrophysiological properties of two axonal sodium channels, $Na_v1.2$ and $Na_v1.6$, expressed in mouse spinal sensory neurones. J Physiol (Lond) 564:803–815.

Schmid S, Guenther E (1996) Developmental regulation of voltage-activated Na^+ and Ca^{2+} currents in rat retinal ganglion cells. NeuroReport 7:677–681.

Schmid S, Guenther E (1998) Alterations in channel density and kinetic properties of the sodium current in retinal ganglion cells of the rat during in vivo differentiation. Neuroscience 85:249–258.

Smith MR, Smith RD, Plummer NW, Meisler MH, Goldin AL (1998) Functional analysis of the mouse Scn8a sodium channel. J Neurosci 18:6093–6102.

Spampanato J, Escayg A, Meisler MH, Goldin AL (2001) Functional effects of two voltage-gated sodium channel mutations that cause generalized epilepsy with febrile seizures plus type 2. J Neurosci 21:7481–7490.

Trimmer JS, Rhodes KJ (2004) Localization of voltage-gated ion channels in mammalian brain. Annu Rev Physiol 66:477–519.

Trudeau MM, Dalton JC, Day JW, Ranum LP, Meisler MH (2005) Heterozygosity for a protein truncation mutation of sodium channel SCN8A in a patient with cerebellar atrophy, ataxia and mental retardation. J Med Genet 43:527–530.

Usrey WM, Reppas JB, Reid RC (1998) Paired-spike interactions and synaptic efficacy of retinal inputs to the thalamus. Nature 395:384–387.

Van Wart A, Boiko T, Trimmer JS, Matthews G (2004) Sodium channels $Na_v1.1$ and $Na_v1.6$ are differentially targeted within the axon initial segment of retinal ganglion cells. Soc Neurosci Abstr 31:397.13.

Van Wart A, Boiko T, Trimmer JS, Matthews G (2005) Novel clustering of sodium channel Na_v 1.1 with ankyrin-G and neurofascin at discrete sites in the inner plexiform layer of the retina. Mol Cell Neurosci 28:661–673.

Velte TJ, Masland RH (1999) Action potentials in the dendrites of retinal ganglion cells. J Neurophysiol 81:1412–1417.

Voigt T, Wässle H (1987) Dopaminergic innervation of A II amacrine cells in mammalian retina. J Neurosci 7:4115–4128.

Völgyi B, Abrams J, Paul DL, Bloomfield SA (2005) Morphology and tracer coupling pattern of alpha ganglion cells in the mouse retina. J Comp Neurol 492:66–77.

Wang GY, Ratto G, Bisti S, Chalupa LM (1997) Functional development of intrinsic properties in ganglion cells of the mammalian retina. J Neurophysiol 78:2895–2903.

Zaghloul KA, Boahen K, Demb JB (2003) Different circuits for ON and OFF retinal ganglion cells cause different contrast sensitivities. J Neurosci 23:2645–2654.

Zhou W, Goldin AL (2004) Use-dependent potentiation of the $Na_v1.6$ sodium channel. Biophys J 87:3862–3872.